

1 Treatment Planning for Patients with Multiple Lung Disease Sites

1.1 Introduction

Lung cancer is the leading cause of cancer-related death, with approximately 160 000 deaths in the U.S. in 2014 [Siegel et al., 2014]. More than half of all patients with lung cancer are diagnosed with stage IV non-small cell lung cancer (NSCLC) [Ramalingam and Belani, 2008, Iyengar et al., 2014]. Prognosis for stage IV NSCLC is poor, with only 12 months median survival after first line chemotherapy [Socinski et al., 2013].

Stereotactic body radiation treatment (SBRT) shows good results for treating NSCLC [Baumann et al., 2009, Fakiris et al., 2009, Grutters et al., 2010, Greco et al., 2011]. Furthermore, several studies have shown that SBRT can be used in the setting of limited metastatic disease [?, ?, Salama et al., 2012, Iyengar et al., 2014]. Passive scattering particle therapy has also proved as an effective treatment for NSCLC [Grutters et al., 2010, Tsujii and Kamada, 2012] and it could be considered an alternative to photon treatment.

It was shown in Chapter ?? that scanned carbon ions (PT) could also be used as a treatment modality for NSCLC. One of the conclusions of the study shown in Chapter ?? was that patients with multiple disease sites would especially benefit from PT compared to SBRT. However, limitations of this study were small number of patients (4) and single-field uniform optimization (SFUD) used in treatment planning. Since patients with multiple metastases present complex geometry, clinically acceptable treatment plans can not be created with SFUD. Intensity modulated particle therapy (IMPT), on the other hand, should get an adequate treatment plans.

An investigation of IMPT with state of the art 4D optimization for treating lung cancer patients with multiple disease sites was made. Treatment plans were generated with two different 4D optimization techniques and compared with SBRT plans, which were actually used for treating patients.

1.2 Materials and Methods

For creation of treatment plans 4D extension of GSI's treatment planning system TRiP98 [Krämer and Scholz, 2000, Richter et al., 2013] was used and modified. A description of modifications and tools used will be given here, alongside with patient data.

1.2.1 Patient data

In this study, 8 patients with 2 - 5 lung metastases summing to 24 metastases in total were included. The lesion size was 4.2 cm^3 (median, 25-75% 2.4 - 22.2) and peak-to-peak motion was 5.9 mm (2.7 - 8.1). Details are given in Table 1.1. Target motion and PT treatment planning were based on a 4D-CT, consisting of 10 phases (0 - 9), with phase 0 (end-inhale) chosen as a reference phase. A registered positron emission tomography (PET) scan was used to delineate clinical target volumes (CTV).

Patients 1 - 4 had no OARs in CTV vicinity (closer than 10 mm) and patients 5 - 8 had at least one OAR in CTV vicinity (closer than 10 mm).

Patients were treated with SBRT at Chamaplimaud Center for the Unknown, Lisbon (Portugal), with different fraction schemes. Number of fractions and doses delivered are given in Table 1.1.

1.2.2 Multiple targets

The TRiP98 optimization works on minimizing residual of a nonlinear equation system [Krämer and Scholz, 2000]. The minimizing function $E(\vec{N})$ for particle number \vec{N} goes as:

$$E(\vec{N}) = \sum_{i \in T} \left(D_{pre}^i - D_{act}^i(\vec{N}) \right) = \sum_{i \in T} \left(D_{pre}^i - \sum_{j=1}^n c_{ij} N_j \right) \quad (1.1)$$

For a CT voxel i in target T , D_{pre} and D_{act} are the prescribed and the actual dose, respectively. The coefficient c_{ij} stands for correlation between dose deposition and field position j at a voxel i , with n the number of fields. There is no restriction for the number of targets or fields in the minimizing function, so it can be expanded to:

$$E(\vec{N}) = \sum_T \sum_{i \in T} \left(D_{pre}^i - \sum_{j=1}^n c_{ij} N_j \right) \quad (1.2)$$

However, the setup of raster points in TRiP98 allowed only one target. It was therefore expanded in a way that a field was designated to a specific target, as displayed in Fig 1.1.

Raster points for each field are created only around designated target. Contribution from all fields are then calculated in optimization. When a field from one target contributes dose to the other target this is taken into account in optimization function, specifically in coefficient c_{ij} in Eq. 1.3. Because the optimization function was not changed, all TRiP98 4D functionalities could be used, as explained in next sections.

Table 1.1: Target characteristics, with CTV volumes, peak-to-peak motions, fractionation schemes and number of fields used for PT treatment planning. Last column shows an OAR in target vicinity (closer than 10 mm), if present. SA stands for smaller airways and esoph. for esophagus.

Patient	Target	Volume (cm ³)	Peak-to-peak motion [mm]	Fractionation scheme	Number of fields	OAR in proximity
1	a	10.2	3.4	1 x 24 Gy	2	SA
	b	14.4	2.8	1 x 24 Gy	2	
2	a	3.8	5.8	1 x 24 Gy	2	
	b	4.3	0.8	1 x 24 Gy	2	
	c	2.7	3.4	1 x 24 Gy	2	
	d	3.1	2.1	1 x 24 Gy	2	
	e	0.5	0.5	1 x 24 Gy	2	
3	a	139	0.6	1 x 24 Gy	3	
	b	9.2	2.0	1 x 24 Gy	2	
4	a	4	9	3 x 9 Gy	5	SA, esoph., heart
	b	0.8	7.8	1 x 24 Gy	2	
5	a	3.4	5	1 x 24 Gy	3	
	b	2.4	4.4	1 x 24 Gy	2	
	c	2.0	6.3	1 x 24 Gy	2	Heart
	d	2.4	6.4	1 x 24 Gy	2	Heart
6	a	20.6	7.4	1 x 24 Gy	4	SA
	b	27.1	6.0	1 x 24 Gy	4	SA
7	a	2.3	12	1 x 24 Gy	2	Heart, esoph., stomach
	b	0.4	11.8	5 x 7 Gy	4	
8	a	136	12	3 x 9 Gy	2	Heart
	b	12.4	2.5	1 x 20 Gy	2	
	c	123	14	3 x 9 Gy	2	Heart
	d	80.7	17	1 x 22 Gy	3	
	e	86.7	6.6	1 x 20 Gy	3	SA

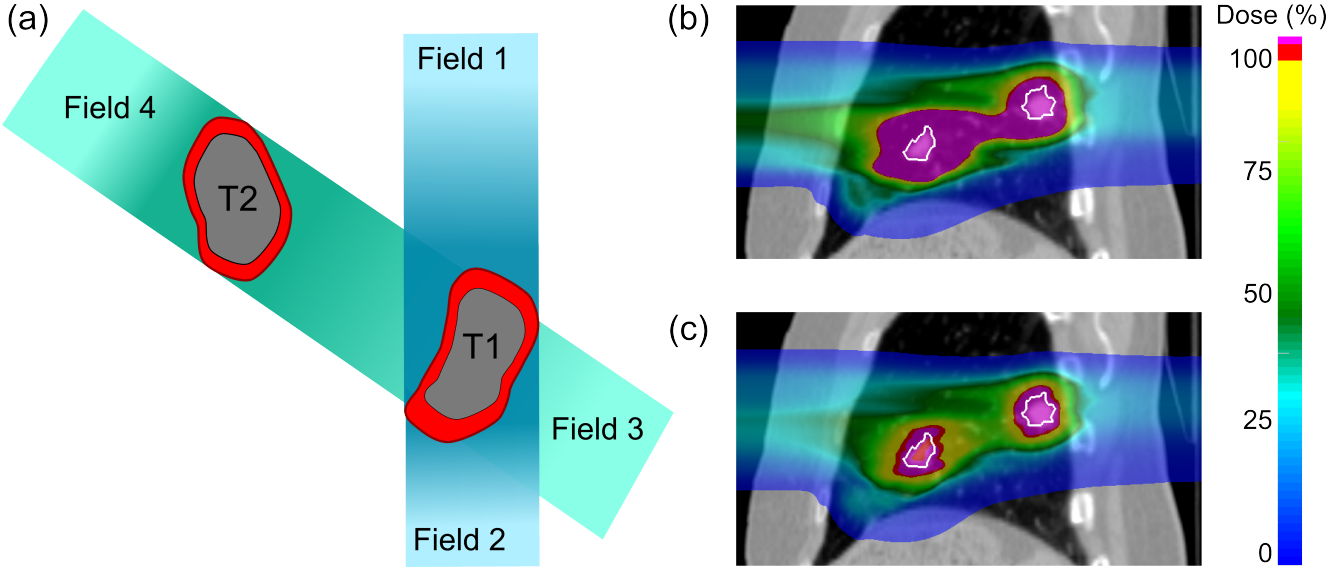


Figure 1.1: Optimization of multiple targets. (a) Fields 1 and 2 are designated to target T1 and fields 3 and 4 to target T2. Optimization takes into account all target voxels and contributions from all fields. An example is shown in (b) and (c), where targets were optimized individually (b) and together (b). The dose in (b) reaches almost 200%.

1.2.3 Optimization techniques

Investigation of two different optimization techniques to handle range changes in moving tumors was made. For each patient, two sets of plans were created: field-independent ITV (ITV) and 4D optimization (4Dopt).

- **Field-independet ITV:** A water-equivalent path length ITV (WEPL-ITV) is different for each field, creating unnecessary margins when combining WEPL-ITV from different fields (see Fig. 1.2a). Graeff et. al [Graeff et al., 2012] proposed a solution to include range margin into the field description itself, instead of creating a bigger PTV. Thus, no unnecessary margins are created. Treatment plans were made for all targets with intensity IMPT on a ITV in reference phase.
- **4D Optimization:** IMPT with ITV can produce inhomogeneous fields that yield homogeneous dose but only in reference phase. The WEPL can change in different motion phases, leading to inhomogeneous dose. 4Dopt uses WEPL-ITV for raster setup, however the actual optimization is performed on each target voxel in each motion state k . The optimization function thus changes to [Graeff et al., 2012]:

$$E(\vec{N}) = \sum_{k=1}^m \sum_{T_k} \sum_{i \in T_k} \left(D_{pre}^i - \sum_{j=1}^n c_{ijk} N_j \right) \quad (1.3)$$

All targets were treated with IMPT and 4D optimization. A subset of motion states 0, 5 and 7% was used for targets 6a - d, 7b, 8a and 8c due to large optimization problem - beside multiple targets, OAR was also included in motion states [Graeff et al., 2012].

The same number of fields and the same field angles were used in both techniques.

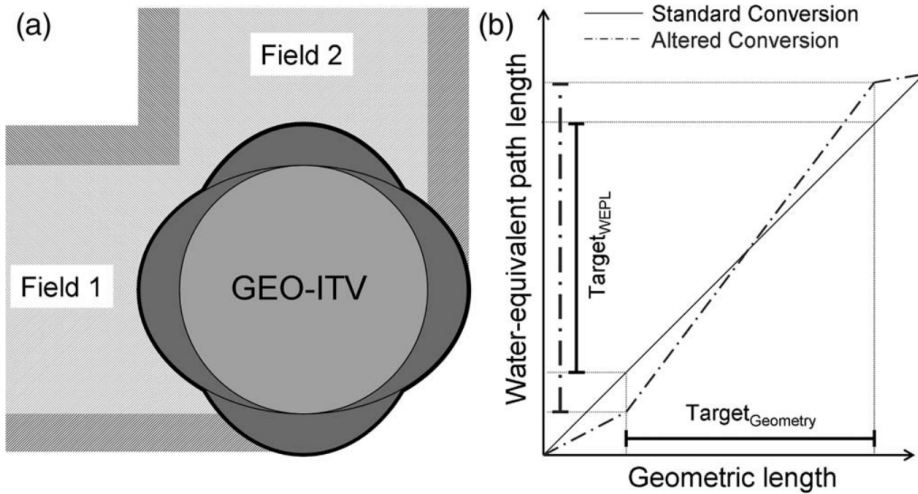


Figure 1.2: Schematic presentation of the ITV. (a) Dark gray ellipses show margins needed for specific fields to account for range changes in different motion states. When common target volume for two perpendicular fields is generated (this black contour) it creates unnecessary lateral extension of both fields, as shown by the dark gray entry channels. A solution is shown in (b). Rather than using standard, geometric, margins, both fields use the same geometry, however the conversion of geometry to WEPL is altered for each field. The plot in (b) shows the standard (solid line) and an altered conversion (dashed-dotted line) for a beam passing a homogeneous CTV. The altered conversion increases the WEPL extent and thus implicitly increasing margins for a single field only. Figure taken from [Graeff et al., 2012]

1.2.4 Treatment planning

An isotropic margin of 3 mm was added to each CTV to account for uncertainties in treatment delivery. An WEPL-ITV was constructed on the CTV with margins for each individual field, which was then used either in optimization (inITV) or for raster setup (4Dopt). Due to large memory demands, targets in each lung were optimized separately.

The objective for target was 99% of each target volume should receive at least 100% of the planned dose ($D_{99\%} \geq 100\%$). Furthermore, the doses to the OARs should be under the limits given by the AAPM task group [Benedict et al., 2010].

After the optimization 4D-dose was calculated for two motion periods (3.6 sec and 5.0 sec) and two starting phases (0° and 90°) as explained in Section ???. The relative biological effectiv-

ness (RBE) was calculated with local effect model, LEM IV [?]. Alpha beta ratio of 6 and 2 was used in target and normal tissue, respectively.

Motion was mitigated by applying slice-by-slice rescanning to each plan. The number of rescans was limited by the number of particles in a single raster point, which should not be lower than 8000, due to the monitoring precision. The maximum number of rescans was limited to 20.

Detailed explanation of SBRT treatment planning is given in Section ??.

For patients 4 - 7 OAR dose could not be sufficiently reduced in optimization. It was necessary to add margins to the OAR and then subtract the OAR plus margins from the target. For SBRT the OAR plus margins was subtracted from PTV, while in PT it was subtracted from CTV plus 3 mm margin in all 9 motion states.

1.2.5 Fractionation escalation

A single fraction of 24 Gy could not be used in SBRT treatment for targets 4a, 7b and 8a-e due to the OAR dose constraints. For these targets additional PT plans were generated with 1 x 24 Gy fractionation scheme, in order to estimate if PT could respect OAR constraints for these targets.

1.3 Results

Example of different treatment plans for patient 2 is shown in Fig. 1.3.

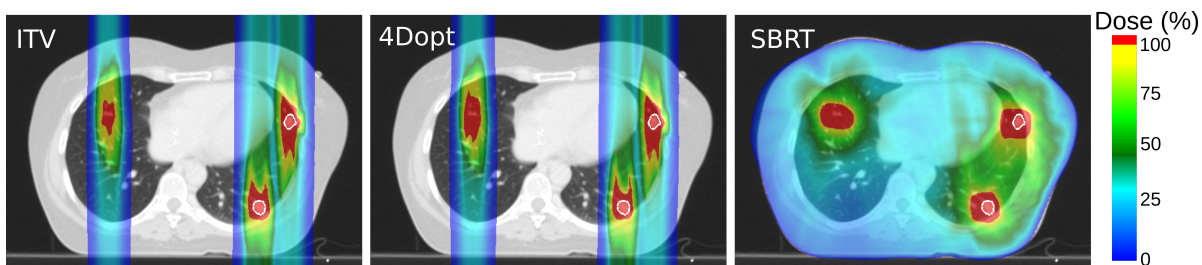


Figure 1.3: Treatment plans for ITV (left), 4Dopt (middle) and SBRT (right) for SBRT (solid lines) for patient 2. CTV contours are outlined in white.

1.3.1 Target Coverage

Results for CTV $D_{99\%}$ for all patients are shown in Table 1.2. All SBRT plans were approved by a physician, even though the prescription dose for patients 5 - 7 was not met due to an OAR proximity. Excluding patients 5 - 7, there were 8 cases (out of 20) of too low CTV dose across different motion types for ITV and 4Dopt, respectively. The lowest CTV $D_{99\%}$ was 86.5%. For

patients 6 - 8 ITV and 4Dopt had higher CTV $D_{99\%}$ than SBRT, except for target 7c. There was no significant difference in CTV $D_{99\%}$ between SBRT, ITV and 4Dopt.

Table 1.2: CTV $D_{99\%}$ for ITV, 4Dopt and SBRT for 8 patients. Results for ITV and 4Dopt are shown as median (range) across different motion types.

Patient	Target	CTV $D_{99\%}$ (%)		
		ITV	4Dopt	SBRT
1	a	101.6(100.0 - 102.1)	101.0(101.0 - 101.0)	100.0
	b	101.6(101.0 - 102.1)	102.1(101.0 - 102.1)	100.0
1	a	101.0(100.0 - 101.0)	100.5(100.0 - 101.0)	101.0
	b	107.1(103.6 - 107.1)	100.0(100.0 - 103.6)	100.0
1	a	101.0(99.0 - 102.1)	99.0(99.0 - 102.1)	106.3
	b	102.1(99.0 - 102.1)	102.1(102.1 - 102.1)	103.1
	c	101.0(101.0 - 102.1)	101.6(101.0 - 102.1)	104.2
	d	102.1(99.0 - 102.1)	101.6(101.0 - 102.1)	107.3
	e	102.1(102.1 - 102.1)	102.1(101.0 - 102.1)	108.3
1	a	102.1(102.1 - 102.1)	102.1(102.1 - 102.1)	101.0
	b	99.0(99.0 - 99.0)	100.0(100.0 - 101.0)	102.1
1	a	64.4(63.9 - 64.8)	74.5(74.1 - 75.9)	66.7
	b	100.5(99.0 - 102.1)	100.5(99.0 - 102.1)	103.1
1	a	100.5(100.0 - 102.1)	99.5(99.0 - 101.0)	101.0
	b	100.5(100.0 - 101.0)	100.0(100.0 - 100.0)	101.0
	c	91.1(88.5 - 92.7)	92.7(86.5 - 93.8)	99.0
	d	97.4(93.8 - 100.0)	100.0(99.0 - 101.0)	94.8
1	a	87.5(86.5 - 89.6)	94.3(92.7 - 94.8)	69.8
	b	79.7(79.2 - 81.3)	78.6(77.1 - 79.2)	69.8
1	a	100.9(100.0 - 100.9)	99.5(99.1 - 100.9)	105.6
	b	100.0(98.8 - 101.3)	102.5(101.3 - 102.5)	105.0
	c	99.1(99.1 - 100.0)	99.5(97.2 - 100.0)	106.5
	d	102.3(100.0 - 104.5)	100.6(100.0 - 101.1)	102.3
	e	101.9(101.3 - 102.5)	102.5(101.3 - 102.5)	101.3

1.3.2 Dose in OARs

D_{Max} and D_{Mean} for 8 OARs are shown in Table 1.3. There was a significant difference between PT and SBRT in D_{Max} and D_{Mean} for heart, spinal cord, esophagus and aorta and in D_{Mean} for smaller airways and ipsilateral lung. No significant difference was observed in dose to OAR between different motion types or between ITV and 4Dopt. The overall OAR difference for patients between SBRT and mITV was significant, 3.1 Gy (0.5 - 7.9) for D_{Max} and 1.7 Gy (0.7 - 3.0) for D_{Mean} . There was no significant difference between mITV and 4DITV to overall dose to OAR. The ipsilateral lung $V_{20\%}$ was 14.4 (0.0 - 43.0), 14.6 (0.0 - 41.4) and 29.8 (5.8 - 89.2)% for

mITV, ITV and SBRT, respectively. Both, mITV and 4DITV ipsilateral lung $V_{20\%}$ was significantly different from SBRT, while no significant difference was observed between mITV and 4DITV.

Dose volume histograms (DVH) for patients 5 - 8 are shown in Fig. 1.4. The margins used for OAR subtraction for PT and SBRT, respectively, were: 3 and 5 mm for smaller airways, 0 and 1 mm for esophagus in patient 5; 0 and 2 mm for heart in patient 6; 2 and 11 mm for smaller airways in left lung, 0 and 9 mm for smaller airways in right lung.

All treatment plans exceeded the D_{Max} limit for smaller airways in patients 5, 7 and 8 and for heart in patient 7. Additionally, SBRT Esophagus and Heart D_{Max} limits were exceeded in patients 5 and 8, respectively.

Table 1.3: OAR D_{Max} and D_{Mean} of all patients for ITV, 4Dopt and SBRT. There was significant difference between PT and SBRT for all OARs, except smaller airways' D_{Max} . Data is displayed as median (range).

OAR	ITV	4Dopt	SBRT
D_{Max} (Gy)			
heart	13.9(0.0 - 28.5)	14.6(0.0 - 29.3)	18.1(7.5 - 30.5)
spinalcord	0.4(0.0 - 8.3)	0.3(0.0 - 8.5)	9.0(3.0 - 12.5)
smallerairways	11.6(0.0 - 21.3)	11.5(0.0 - 22.8)	15.6(0.0 - 22.8)
esophagus	0.6(0.0 - 23.0)	0.9(0.0 - 23.3)	11.5(5.5 - 25.5)
aorta	4.4(0.0 - 28.5)	6.3(1.5 - 26.5)	18.1(6.3 - 31.0)
Ipsilateral lung	26.6(0.0 - 31.5)	26.1(0.3 - 29.8)	26.1(3.8 - 32.3)
D_{Mean} (Gy)			
heart	0.3(0.0 - 0.8)	0.4(0.0 - 0.8)	4.4(2.5 - 10.1)
spinalcord	0.0(0.0 - 0.5)	0.0(0.0 - 0.6)	1.8(0.8 - 2.5)
smallerairways	1.1(0.0 - 5.6)	1.2(0.0 - 7.3)	3.5(0.0 - 7.5)
esophagus	0.1(0.0 - 1.3)	0.1(0.0 - 1.4)	3.3(1.4 - 5.1)
aorta	0.3(0.0 - 1.0)	0.4(0.0 - 0.8)	2.9(1.3 - 6.2)
Ipsilateral lung	2.2(0.0 - 9.1)	2.3(0.0 - 8.6)	4.1(0.8 - 10.5)

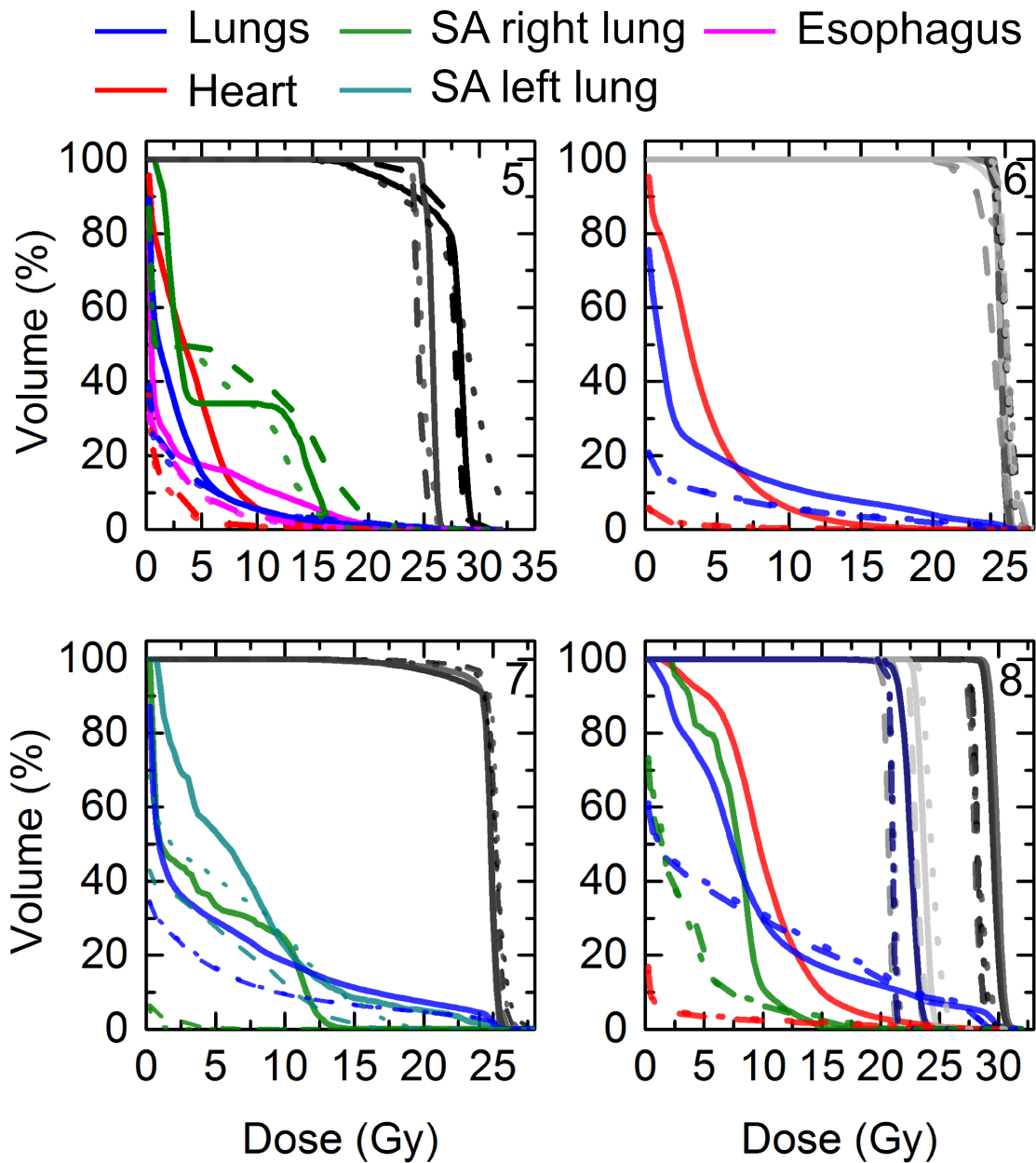


Figure 1.4: Dose volume histograms for patients 5 -8. SBRT, mITV and 4DITV are represented by solid, dashed and dotted line, respectively. Targets are displayed in grayscale, while OAR use colors shown above. SA stands for smaller airways.

1.3.3 Fractination escalation

With PT the 1×24 Gy fractionation scheme could be used for targets 8a-e, violating only D_{Max} for smaller airways. SBRT limitation was $D_{Threshold}$ which was 100% of the allowed dose, whereas for PT it was 45%. For targets 4a and 7b the CTV $D_{99\%}$ was 70% and 81% and esophagus D_{Max} 125% and 143% respectively. The esophagus D_{Max} was the only violation of OAR constraints.

1.4 Summary and Discussion

Clinically valid SBRT plans have been compared to PT treatment plans for NSCLC patients with multiple metastases. To the best of our knowledge, this is the first study of treating multiple NSCLC metastases with PT. Novel approach was used to handle multiple targets, together with the state of the are 4D PT treatment planning. Furthermore, 4D PT doses were calculated for different motion types.

PT on average delivered less dose to OAR, while still having comparable target coverage. The most apparent difference is in lung $V_{20\%}$, which was on average half the value with PT compared to SBRT. For patients with complex geometry (4 - 8) PT maintained or even improved target coverage in most cases, while reducing doses to OARs. The exception were smaller airways in patients 4, which receive more dose, but the CTV $D_{99\%}$ was improved. Additionally, margins used for OAR subtraction were smaller in PT, resulting in better CTV coverage.

There was no significant difference between ITV and 4Dopt in target coverage or in dose to OAR. However, in patients 5 and 7 the 4Dopt was able to achieve better target coverage. With ITV, patient 5 had extreme inhomogeneous target coverage, resulting in lung $D_{Max} = 32.5$ Gy, compared to 29.3 Gy and 29.8 Gy with 4Dopt and SBRT, respectively. For patient 7, 4Dopt deposited less dose to smaller airways in addition to better target coverage.

For patient 8 the fractionation scheme could be changed to 1×24 Gy , which had the largest total target volume. SBRT had to change the fractionation scheme due to large heart dose, which PT could reduce with narrow entry channel. For targets 4a and 7b the fractionation scheme could not be changed, due too high esophagus D_{Max} . Furthermore, the D_{Max} esophagus constraint was violated even in 5×7 Gy fractionation scheme with PT - it was 105% adn 104% for ITV and 4Dopt, respectively. The reason lies in the large target motion (12

Even though PT deposits less dose to OAR with the same or even better target coverage, there is still room for improvement in PT 4D treatment planning. An implementation of multi-criteria objective planning should bring even better dose distribution and bring possibility to choose between trade-offs [Breedveld et al., 2007, Chen et al., 2010]. Additionally, multiple target optimization in PT would benefit from a shell around PT where dose would be minimized. Therefore excessive dose in healthy tissue would be further reduced. An introduction of a shell,

however, would further enlarge the optimization problem, which is big already for complex geometry (patient 5 - 8). A possible solution for minimizing voxel number in optimization would be with adaptive dose grid [?].

In Chapter ?? additional range margins to account for range uncertainties could be used in treatment planning, due to SFUD. Because we did not use field specific PTVs it was not possible to include range uncertainties in our study. Instead of creating field specific PTVs to include range uncertainties, a solution was proposed to include uncertainties in optimization process itself [Pflugfelder et al., 2008, Unkelbach et al., 2009, Fredriksson et al., 2011, Chen et al., 2012]. Chen et al. have shown it is possible to implement robust optimization in multi-criteria optimization as well [Chen et al., 2012]. Furthermore, in a recent treatment planning study by Liu et al. [Liu et al., 2016] a 4D robust optimization was demonstrated, with better results over 3D robust optimization for NSCLC patients. However, only breathing starting phase was used as an uncertainty, whereas different motion types should be considered. The disadvantage of 3D and 4D robust optimization is the enlargement of the optimization problem.

Patient 6 D_{Max} heart dose ranged over 2 Gy across different motion types in 4Dopt, showing the necessity of making treatment plans robust against motion uncertainty, especially in the hypo-fractionated regimen. Furthermore, the doses to OARs that are under the limits after optimization, may exceed them after calculating 4D dose. The ITV and 4Dopt approaches take into account range changes in different motion states, however they do not guarantee 4D doses. This could be achieved with beam tracking [?], when each motion state has designated treatment plan. Clinical application of beam tracking is not yet feasible due to several reasons, such as the inverse interplay, the ion-beam tracking system complexity, precision and speed of the motion monitoring. Another solution would be jet-ventilation [?], however, it brings additional complications to treatment.

Apart from 4D robust optimization, the effect of motion could be minimized by using other motion mitigation techniques, such as gating. Furthermore, gating could improve the target coverage, where the planned dose was not met. Gating, together with rescanning, has already been successfully implemented clinically for active beam scanning [Rossi, 2016, Mori et al., 2016] and it might be essential to use it in hypo-fractionated treatment of moving tumors.

A recent review showed good local control rates between 66 - 92% for patients treated with SBRT in reoccurred tumors in previous irradiation field [Amini et al., 2014]. However, there were grade 4 and 5 complications present, i.e. study by Trovo et al showed grade 5 pneumonia in 6% of patient treated [Trovo et al., 2014]. As shown in our study, PT delivers less dose to the OAR, ipsilateral lung in particular, and could hence reduce the number of treatment-related complications.

1.5 Conclusions

PT delivers less dose to OAR compared to SBRT in NSCLC patients with multiple disease sites, while maintaining the same target coverage. Caution has to be taken in patients with OAR in CTV vicinity (less than 10 mm), where doses to OAR differ across different motion types. No significant difference was found between two 4D optimization techniques. However, 4D optimization showed better results for patients with OAR in CTV vicinity.

Bibliography

- [Amini et al., 2014] Amini, A., Yeh, N., Gaspar, L. E., Kavanagh, B., and Karam, S. D. (2014). Stereotactic body radiation therapy (sbrt) for lung cancer patients previously treated with conventional radiotherapy: a review. *Radiation Oncology*, 9(1):1–8.
- [Baumann et al., 2009] Baumann, P., Nyman, J., Hoyer, M., Wennberg, B., Gagliardi, G., Lax, I., Drugge, N., Ekberg, L., Friesland, S., Johansson, K. A., Lund, J. A., Morhed, E., Nilsson, K., Levin, N., Paludan, M., Sederholm, C., Traberg, A., Wittgren, L., and Lewensohn, R. (2009). Outcome in a prospective phase ii trial of medically inoperable stage i non-small-cell lung cancer patients treated with stereotactic body radiotherapy. *Journal of Clinical Oncology*, 27(20):3290–3296.
- [Benedict et al., 2010] Benedict, S. H., Yenice, K. M., Followill, D., Galvin, J. M., Hinson, W., Kavanagh, B., Keall, P., Lovelock, M., Meeks, S., Papiez, L., Purdie, T., Sadagopan, R., Schell, M. C., Salter, B., Schlesinger, D. J., Shiu, A. S., Solberg, T., Song, D. Y., Stieber, V., Timmerman, R., Tome, W. A., Verellen, D., Wang, L., and Yin, F. F. (2010). Stereotactic body radiation therapy: the report of aapm task group 101. *Medical Physics*, 37(8):4078–4101.
- [Bert and Rietzel, 2007] Bert, C. and Rietzel, E. (2007). 4D treatment planning for scanned ion beams. *Radiat. Oncol.*, 2(24).
- [Breedveld et al., 2007] Breedveld, S., Storchi, P. R. M., Keijzer, M., Heemink, A. W., and Heijmen, B. J. M. (2007). A novel approach to multi-criteria inverse planning for imrt. *Physics in Medicine and Biology*, 52(20):6339.
- [Chen et al., 2010] Chen, W., Craft, D., Madden, T. M., Zhang, K., Kooy, H. M., and Herman, G. T. (2010). A fast optimization algorithm for multicriteria intensity modulated proton therapy planning. *Med Phys*, 37(9):4938–4945.
- [Chen et al., 2012] Chen, W., Unkelbach, J., Trofimov, A., Madden, T., Kooy, H., Bortfeld, T., and Craft, D. (2012). Including robustness in multi-criteria optimization for intensity-modulated proton therapy. *Physics in Medicine and Biology*, 57(3):591–608.
- [Elsaesser et al., 2010] Elsaesser, T., Weyrather, W. K., Friedrich, T., Durante, M., Iancu, G., Krämer, M., Kragl, G., Brons, S., Winter, M., Weber, K. J., and Scholz, M. (2010). Quantification of the relative biological effectiveness for ion beam radiotherapy: direct experimental comparison of proton and carbon ion beams and a novel approach for treatment planning. *Int. J. Radiat. Oncol. Biol. Phys.*, 78(4):1177–1183.

- [Fakiris et al., 2009] Fakiris, A. J., McGarry, R. C., Yiannoutsos, C. T., Papiez, L., Willams, M., Henderson, M. A., and Timmerman, R. (2009). Stereotactic body radiation therapy for early-stage non-small-cell lung carcinoma: four-year results of a prospective phase ii study. *International Journal of Radiation Oncology*, 75(3):677–682.
- [Fredriksson et al., 2011] Fredriksson, A., Forsgren, A., and Hårdemark, B. (2011). Minimax optimization for handling range and setup uncertainties in proton therapy. *Medical Physics*, 38(3):1672–1684.
- [Graeff et al., 2012] Graeff, C., Durante, M., and Bert, C. (2012). Motion mitigation in intensity modulated particle therapy by internal target volumes covering range changes. *Medical Physics*, 39(10):6004–6013.
- [Greco et al., 2011] Greco, C., Zelefsky, M. J., Lovelock, M., Fuks, Z., Hunt, M., Rosenzweig, K., Zatcky, J., Kim, B., and Yamada, Y. (2011). Predictors of local control after single-dose stereotactic image-guided intensity-modulated radiotherapy for extracranial metastases. *Int.J.Radiat.Oncol.Biol.Phys.*, 79(4):1151–1157.
- [Grutters et al., 2010] Grutters, J. P. C., Kessels, A. G. H., Pijs-Johannesma, M., Ruysscher, D., oore, M. A. ., and Lambin, P. (2010). Comparison of the effectiveness of radiotherapy with photons, protons and carbon-ions for non-small cell lung cancer: A meta-analysis. *Radiotherapy and Oncology*, 95(1):32–40.
- [Iyengar et al., 2014] Iyengar, P., Kavanagh, B. D., Wardak, Z., Smith, I., Ahn, C., Gerber, D. E., Dowell, J., Hughes, R., Camidge, D. R., Gaspar, L. E., Doebele, R. C., Bunn, P. A., Choy, H., and Timmerman, R. (2014). Phase ii trial of stereotactic body radiation therapy combined with erlotinib for patients with limited but progressive metastatic non-small-cell lung cancer. *J.Clin.Oncol.*, 32(34):3824–3854.
- [Krämer and Scholz, 2000] Krämer, M. and Scholz, M. (2000). Treatment planning for heavy-ion radiotherapy: calculation and optimization of biologically effective dose. *Phys. Med. Biol.*, 45(11):3319–3330.
- [Liu et al., 2016] Liu, W., Schild, S. E., Chang, J. Y., Liao, Z., Chang, Y.-H., Wen, Z., Shen, J., Stoker, J. B., Ding, X., Hu, Y., Sahoo, N., Herman, M. G., Vargas, C., Keole, S., Wong, W., and Bues, M. (2016). Exploratory study of 4d versus 3d robust optimization in intensity modulated proton therapy for lung cancer. *International Journal of Radiation Oncology*, 95(1):523–533.
- [Mori et al., 2016] Mori, S., Karube, M., Shirai, T., Tajiri, M., Takekoshi, T., Miki, K., Shiraishi, Y., Tanimoto, K., Shibayama, K., Yasuda, S., Yamamoto, N., Yamada, S., Tsuji, H., Noda, K.,

- and Kamada, T. (2016). Carbon-ion pencil beam scanning treatment with gated markerless tumor tracking: An analysis of positional accuracy. *International Journal of Radiation Oncology*, 95(1):258–266.
- [Pflugfelder et al., 2008] Pflugfelder, D., Wilkens, J. J., and Oelfke, U. (2008). Worst case optimization: a method to account for uncertainties in the optimization of intensity modulated proton therapy. *Phys Med Biol*, 53(6):1689–1700.
- [Prall1 et al., 2016] Prall1, M., Hild, S., Anderle, K., and Graeff, C. (2016). Treatment planning with an adaptive dose grid. In *Abstract Book PTCOG 55*.
- [Ramalingam and Belani, 2008] Ramalingam, S. and Belani, C. (2008). Systemic chemotherapy for advanced non-small cell lung cancer: Recent advances and future directions. *The Oncologist*, 13(suppl 1):5–13.
- [Richter et al., 2013] Richter, D., Schwarzkopf, A., Trautmann, J., Kramer, M., Durante, M., Jakel, O., and Bert, C. (2013). Upgrade and benchmarking of a 4d treatment planning system for scanned ion beam therapy. *Medical Physics*, 40(5):051722.
- [Rossi, 2016] Rossi, S. (2016). The national centre for oncological hadrontherapy (cnao): Status and perspectives. *Physica Medica: European Journal of Medical Physics*, 31(4):333–351.
- [Rusthoven et al., 2009] Rusthoven, K. E., Kavanagh, B. D., Burri, S. H., Chen, C., Cardenes, H., Chidel, M. A., Pugh, T. J., Kane, M., Gaspar, L. E., and Schefter, T. E. (2009). Multi-institutional phase i/ii trial of stereotactic body radiation therapy for lung metastases. *Journal of Clinical Oncology*, 27(10):1579–1584.
- [Salama et al., 2012] Salama, J. K., Hasselle, M. D., Chmura, S. J., Malik, R., Mehta, N., Yenice, K. M., Villaflor, V. M., Stadler, W. M., Hoffman, P. C., Cohen, E. E. W., Connell, P. P., Haraf, D. J., Vokes, E. E., Hellman, S., and Weichselbaum, R. R. (2012). Stereotactic body radiotherapy for multisite extracranial oligometastases. *Cancer*, 118(11):2962–2970.
- [Santiago et al., 2013] Santiago, A., Jelen, U., Ammazzalorso, F., Engenhart-Cabillic, R., Fritz, P., Mühlnickel, W., Enghardt, W., Baumann, M., and Wittig, A. (2013). Reproducibility of target coverage in stereotactic spot scanning proton lung irradiation under high frequency jet ventilation. *Radiotherapy and Oncology*, 109(1):45–50.
- [Siegel et al., 2014] Siegel, R., Ma, J., Zou, Z., and Jemal, A. (2014). Cancer statistics, 2014. *CA: A Cancer Journal for Clinicians*, 64(1):9–29.
- [Socinski et al., 2013] Socinski, M. A., Evans, T., Gettinger, S., Hensing, T. A., Sequist, L. V., Ireland, B., and Stinchcombe, T. E. (2013). Treatment of stage {IV} non-small cell lung cancer: Diagnosis and management of lung cancer, 3rd ed: American college of chest physicians evidence-based clinical practice guidelines. *Chest*, 143(5, Supplement):e341S – e368S.

- [Trovo et al., 2014] Trovo, M., Minatel, E., Durofil, E., Polasel, J., Avanzo, M., Baresic, T., Bearz, A., Del Conte, A., Franchin, G., Gobitti, C., Rumeileh, I. A., and Trovo, M. G. (2014). Stereotactic body radiation therapy for re-irradiation of persistent or recurrent non-small cell lung cancer. *Int J Radiat Oncol Biol Phys*, 88.
- [Tsujii and Kamada, 2012] Tsujii, H. and Kamada, T. (2012). A review of update clinical results of carbon ion radiotherapy. *Jpn.J.Clin.Oncol.*, 42(8):670–685.
- [Unkelbach et al., 2009] Unkelbach, J., Bortfeld, T., Martin, B. C., and Soukup, M. (2009). Reducing the sensitivity of impt treatment plans to setup errors and range uncertainties via probabilistic treatment planning. *Med Phys*, 36(1):149–163. 074812MPH[PII].
- [Villaruz et al., 2012] Villaruz, L. C., Kubicek, G. J., and Socinski, M. A. (2012). Management of non-small cell lung cancer with oligometastasis. *Current Oncology Reports*, 14(4):333–341.